INTERNATIONAL ATOMIC ENERGY AGENCY
UNITED NATIONS EDUCATIONAL, SCIENTIFIC AND CULTURAL ORGANIZATION
INTERNATIONAL CENTRE FOR THEORETICAL PHYSICS
I.C.T.P., P.O. BOX 586, 34100 TRIESTE, ITALY, CABLE CENTRATOM TRIESTE

SMR.703 - 22

WORKING PARTY ON
MECHANICAL PROPERTIES OF INTERFACES

23 AUGUST - 3 SEPTEMBER 1993

"Computer Simulation Techniques Applied to the Study of Interfaces"

V. PONTIKIS
Laboratoire des Solides Irradies
CEA-CEREM, CNRS URA 1380
Ecole Polytechnique
F-91128 Palaiseau Cedex
FRANCE

These are preliminary lecture notes, intended only for distribution to participants.

MAIN BUILDING STRADA COSTIERA, 11 TEL 22401 TELEFAX 224163 TELEX 460392 ADRIATICO GUEST HOUSE VIA GRIGNANO, 9 TEL 22424 TELEFAX 224531 TELEX 460449

Computer simulation techniques applied to the study of interfaces

V. Pontikis

Laboratoire des Solides Irradiés, CEA-CEREM, CNRS URA 1380, Ecole Polytechnique
91128 Palaiseau Cedex, FRANCE

Lecture notes - Working party on Mechanical Properties of Interfaces
August 23 - September 3, 1993, I. A. E. A., I. C. T. P., TRIESTE, ITALY

Contents

I. MC - MD techniques

Realizing the connexion between microscopic and macroscopic properties of matter is an ambition common to several areas in Physics and in Materials Science. The efforts made in recent years in this context rely on the use of digital computers and the associated numerical techniques developed by early work [1-5] are often referred to as simulation techniques. Two types of physical problems are generally handled using simulations: (a) these being by essence probabilistic, due to our partial knowledge of initial conditions or of the mechanisms involved in the process e.g. die games, gallups, population statistical studies and (b) these requiring an estimation of a physical property for systems with a large number of degrees of freedom but having a purely deterministic evolution. Although the term simulation is better adapted to the first class of problems it is also used for the second class to which belong all the questions we focus on in what follows.

Central questions in Materials Science arise from the need of determining thermodynamical properties of perfect and defected systems as well as temperature dependent structural properties (e.g. phase transitions) and the temporal evolution of equilibrium processes (e.g. diffusion mechanisms). Equilibrium properties for a system with given atomic interactions are obtained from statistical thermodynamics in the form of many dimensional integrals over the phase space of the considered system [6]. Since the numerical estimation of such integrals requires a rapidly diverging computational effort [7], simulation techniques i.e. Molecular dynamics and/or Monte Carlo are used to this purpose. These techniques have been employed by many groups to establish the connection between micro and macro "worlds". Their successful application is related to the fact that small system properties, compatible with the limited amount of available computer memory, converge rapidly to their thermodynamical limit values.

Monte Carlo technique

Trough an adequate variable transformation, any integral can in principle be put in the following form :

$$A = \int_0^1 f(X)dX$$

A, representing the area under the curve Y=f(X) displayed on the figure. A Monte Carlo estimation of, A, proceeds as follows:

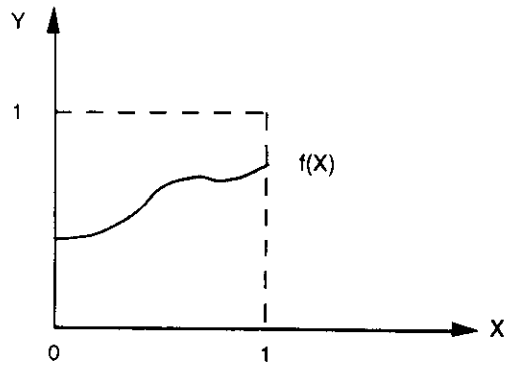

Let us define the random variables X and Y, uniformly distributed over the interval [0,1] and Z such as, Z=1 if Y≤f(X) and Z=0 otherwise. The probability for having Z=1 is simply given by :

$$P(Z=1) = P(Y \le f(X)) = \frac{A}{1 \times 1}$$

For any trial providing a random couple of values (X,Y), p=A and q=1-A are respectively the chances of succes (Z=1) and failure (Z=0). Z is therefore a Bernoulli variable with a binomial distribution of mean, μ=A and variance, σ^2=A(1-A):

$$f(x) = \binom{n}{x} p^x q^{n-x}$$

where, n, is the total number of trials and, x, the number of successful events (Z=1). By defining:

$$\overline{Z}(N) = \sum_{k=1}^{N} Z_k$$

according to Khinchine's theorem, Z(N) converges toward a normaly distributed variable with mean:

$$E(Z(N)) = \frac{1}{N}\sum_{k=1}^{N} E(Z_k) = E(Z_k) = A$$

and variance:

$$\sigma^2 = \frac{var(Z_k)}{N} = \frac{A(1-A)}{N}$$

On the other hand, the distribution function of Z(N) is given by:

$$\rho(Z(N)) = \frac{\sqrt{N}}{\sqrt{2\pi A(1-A)}} \exp\left\{-\frac{N}{2}\left(\frac{Z(N)-A}{\sqrt{A(1-A)}}\right)^2\right\}$$

Let us now estimate the number of trials needed to estimate Z(N), with a given error, ε=|Z(N) -A|. We have:

$$P[|R_N| \le \lambda] = \frac{1}{\sqrt{2\pi}} \int_{-\lambda}^{\lambda} \exp\left(-\frac{R_N^2}{2}\right) dR_N \quad \text{where} \quad R_N = \sqrt{N}\frac{Z(N)-A}{\sqrt{A(1-A)}}$$

and for λ=2 one finds P[|R_N|≤ λ] = 0.95. Solving then the equation |R_N|=2 we obtain:

$$N = \frac{4}{\varepsilon^2} A(1-A)$$

which leads to $N=10^6$ trials if, ε=0.001 and A=0.5. The large value of N thereby obtained, explains why a computer is needed to generate the random variables defined above and to estimate the numerical value of the integral.

The above integral calculation can be of course much more efficiently achieved using standard numerical techniques (e.g. Simpson, Gauss...). However, when dealing with multi-dimensional integrals the computational effort of such methods rises rapidly and the integration is no more feasible. As an example let us consider an integral with 300 variables : if ten values are used for each variable, 10^{300} evaluations of the integrand are needed, a number which obviously exceeds the capabilities of any existing or futur human computing device. This is the problem encountered when thermodynamical properties are needed for a system of N≥100 particles which is being solved using the Monte Carlo technique.

In the example given above, the definition interval of the integrand is sampled uniformly. However, if f(X) is a complicated function as the one schematically drawn in the figure, it appears preferable to sample more often X values for which f(X) values are large. Importance sampling allows the function evaluation to be concentrated in regions of its definition space that make important contributions to the integral. The sampling distribution, $\pi(x)$, should follow as close as possible the variations of f(X). In this case we have:

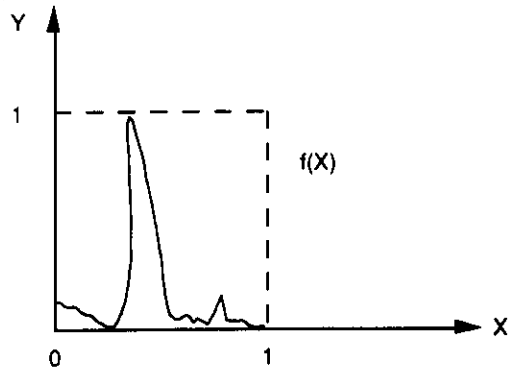

$$I = \int_0^1 f(X)dX = \int_0^1 \left[\frac{f(X)}{\pi(X)}\right]\pi(X)dX \quad \text{and} \quad E\left(\frac{f}{\pi}\right) = \frac{1}{N}\sum_i \left(\frac{f(X_i)}{\pi(X_i)}\right)$$

Let us now consider the computation of thermodynamical averages in the canonical ensemble (NVT). The average value of a given microscopic observable, $A(r_N)$, is defined by [8]:

$$< A >_{NVT} = \frac{\int A(r_N)\exp(-\beta U(r_N))dr_N}{\int \exp(-\beta U(r_N))dr_N}$$

where, $U(r_N)$, is the potential energy function of the considered system. A Monte Carlo evaluation of the integral can be made by sampling configurations from a chosen distribution, ρ, $<A>_{NVT}=<A\rho_{NVT}/\rho>_{trials}$. In the case of functions, $A(r_N)$, varying in the same way as ρ_{NVT}, $\rho=\rho_{NVT}$, will provide a good estimate of the integral. Among existing methods corresponding to such a choice [8], the most widely used is the one devised by Metropolis et al. [9]. However, not all of the thermodynamical quantities can be estimated using importance sampling. An example is provided by the Helmoltz free energy, $F=-k_BT\ln Q_{NVT}$, requiring the evaluation of the integral:

$$Z_{NVT} = \int \exp(-\beta U(r_N))dr_N$$

Consider the identity:

$$\int \left(\frac{\exp(-\beta U(r_N))dr_N}{\int \exp(-\beta U(r_N))dr_N}\right)\exp(\beta U(r_N))dr_N = \frac{V^{3N}}{Z_{NVT}}$$

we then obtain:

$$Z_{NVT} = \frac{V^{3N}}{\int \rho_{NVT}\exp(\beta U(r_N))dr_N}$$

The evaluation of the denominator, $<\exp(bU(r_N))>$, using Metropolis scheme will obviously fail since when the integrand, $\exp(\beta U(r_N))$, reaches increasingly significant values the sampling efficiency decreases due to the shape of the distribution, ρ_{NVT}. Therefore, computations of the free energy require special procedures [10].

Molecular dynamics

An alternative way of sampling the phase space of an N-particle model system, consists in time-integrating the 3N coupled newtonian equations of motion [5]. This is achieved numerically using finite differences schemes one of the most popular being the central difference or Verlet algorithm [4]:

$$r_i(t+\delta t) = 2r_i(t) - r_i(t-\delta t) + \frac{F_i(t)}{m_i}\delta t^2 + O(\delta t^4) \quad \text{and} \quad v_i(t) = \frac{r_i(t+\delta t) - r_i(t-\delta t)}{2\delta t} + O(\delta t^3)$$

where, $\mathbf{r_i}$, $\mathbf{v_i}$ and $\mathbf{F_i}$, are respectively the positions, velocity and force referring to particle i. The solution of these discretized equations requires initial conditions to be specified, usually provided by the set of positions corresponding to the cristalline state of the considered system and a set of velocities sampled from a maxwelian distribution at a temperature twice as large as the target, thermodynamical equilibrium temperature. For simulated temperatures lower than twice the melting point temperature of the cristal, the integration of the above equations is performed using a time step in the interval, $\delta t \in [10^{-15}, 10^{-14}]$, values corresponding to a fraction of the inverse maximum vibrational frequency in the phonon spectrum of the considered material.

In absence of external forces, the simulation reproduces the microcanonical ensemble distribution of states, (NVE), this implying that total energy and translational velocity should remain constant. The conservation of these quantities during a simulation run testifies for the correct choice of the time step and serves as a test to detect program errors.

The above MD technique has been extended to allow for simulations at constant temperature [11], pressure [12] and stress tensor [13]. Thus, (NVT), (NPT), (NPH) or (NΣT) MD simulation techniques are by now available which permitted the study of thermodynamical phase transitions [13].

The estimation of thermodynamical quantities for a given model system obtained using Molecular Dynamics and Monte Carlo should lead in principle to identical results, provided the system under study is ergodic. This is illustrated by Fig. 1 where the potential energy of an n-body model for copper [14], at T=1000 K, is displayed as a function of MD steps / MC moves. Canonical MD has been used to allow for this comparison to be made [11].

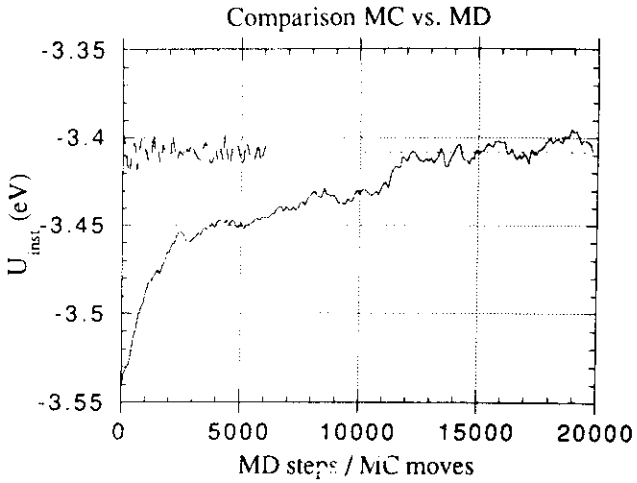

Figure 1 - Potential energy of a N=256 particles model of copper as a function of time steps (canonical MD) or Monte Carlo moves at T=1000 K. Both techniques lead to the same average values.

MD or MC ? is an important question stemming first from relative efficiency considerations of the two methods used in calculations of thermodynamical averages. Usually, MC requires the computation of potential energy differences only. Thus, MC is faster than MD since potential derivatives are not evaluated. However, such a conclusion is not valid when the studied problem involves the computation of stress tensor values. Moreover, the relative efficiency of the two techniques should be estimated at constant variance for the given quantity of interest. It is not clear that MC still preserves a clear advantage over MD in this framework.

In conclusion, MD is used when time dependent quantities are needed e. g. time correlation functions, phase transition or diffusion mechanisms, whereas MC is employed in all other cases. It is also worth to mention that when diffusion dependent phase transitions are simulated, e.g. order-disorder transitions in alloys [15], MC is better adapted than MD in view of an efficient sampling of the phase space to be performed. Indeed, due to the time scale of diffusion events such a transition may never be observed during an MD simulation [15].

The potential is a crucial ingredient of simulations since it determines the stability of the crystalline structure and more generally the properties of the studied system. Before the last decade empirical, pair additive potentials have been used in computer simulations. However, these are not adapted to real materials, e. g. metals, alloys, where n-body effects are of decisive importance. Indeed, pair potentials fail to correctly reproduce surface and bulk dynamical properties [14,16], defect energetics [17] and melting temperatures [14]. Thus, pair potentials are by now used only in generic purpose studies, devoted to the validation of theoretical models, or in special cases such as rare gases and ionic materials where empirical, pair additive potentials (Lennard-Jones (12-6), rigid ion, shell model) still provide a satisfactory description of the real material properties.

The most promising solution for simulations of real material properties are, beyond any doubt, 'ab-initio' methods combining MD or MC techniques and a simultaneous evaluation of energy and forces from first principles. Many variants relying on such an approach have been proposed and tested in recent years [5] among which the first was a combination of MD and density functional theory due to Car and Parrinello [18]. Despite recent developments, such techniques require heavy computations and therefore only small size systems (typically N≈100) are currently studied. Since simulations in materials science often imply the use of large systems ($N \approx 10^4$-10^7), semi-empirical techniques based on the embedded atome method (EAM) [19] or the tight binding (TB) approximation for transition metals [20-22] became popular. These provide n-body potentials that have been widely used to the study of properties of metals and alloys.

Among these potentials, those based on the second moment approximation of the tight binding scheme are the simplest and contain only few adjustable parameters. Thus additional information is given below on this type of n-body potentials, particularly well adapted to the case of transition metals and their alloys.

The cohesive properties of transition metals stem from the large d-electron band density of states. Early work has shown that several properties are determined by the effective d-band width, not on the details of the density of states [20]. Accordingly, the band energy can be written in the following form:

$$E_b^i = -\xi\left\{\sum_{j\neq i}\exp\left[-2q\left(\frac{r_{ij}}{d}-1\right)\right]\right\}^{1/2}$$

where, ξ, is an effective hopping integral, r_{ij}, the distance between sites i and j and d, is usually taken equal to the first neighbors distance. The stability of the system requires also the addition of a repulsive term, often chosen as a Born-Mayer pairwise interaction [17,20]. Thus the total cohesive energy of such a system is given by:

$$E = \sum_i\left\{\sum_{j\neq i} A\exp\left[-p\left(\frac{r_{ij}}{d}-1\right)\right]\right\} - \sum_i \xi\left\{\sum_{j\neq i}\exp\left[-2q\left(\frac{r_{ij}}{d}-1\right)\right]\right\}^{1/2}$$

The parameters A, ξ, p and q, are determined by a multidimensional fit of the above formula to the cohesive energy, the elastic constants and the equilibrium equation of the material of interest. Many different minimization techniques are available in the literature but one among the most flexible and well adapted to this type of fit is the MERLIN portable minimization system [23]. In addition to the above adjustable parameters, the use of such a potential for MD/MC simulations requires also the introduction of a cutoff radius for the interactions which acts as an additional parameter.

As it can be seen from the above given expression, this potential is not of the kind "additive pairs" due to the presence of the square root functional. The n-body feature is however better understood upon examination of the force expression:

$$F_i = -\nabla_i E = -\frac{2Ap}{d}\sum_{j\neq i} A\exp\left[-p\left(\frac{r_{ij}}{d}-1\right)\right]\frac{r_{ij}}{|r_{ij}|} + \frac{\xi q}{d}\frac{\sum_{j\neq i}\exp\left[-2q\left(\frac{r_{ij}}{d}-1\right)\right]\frac{r_{ij}}{|r_{ij}|}}{\left\{\sum_{j\neq i}\exp\left[-2q\left(\frac{r_{ij}}{d}-1\right)\right]\right\}^{1/2}}$$

$$+\frac{\xi q}{d}\sum_{j\neq i}\frac{\exp\left[-2q\left(\frac{r_{ij}}{d}-1\right)\right]\frac{r_{ij}}{|r_{ij}|}}{\left\{\sum_{j\neq i}\exp\left[-2q\left(\frac{r_{ij}}{d}-1\right)\right]\right\}^{1/2}}$$

The force on a given atom does not depend only on interactions with neighbors but also on the neighbor environment as is indicated by the last term in the above equation.

TB potentials provided results in excellent agreement with experimental data for bulk [14,17,24] as well as for surface properties [14,16,17]. Moreover, they reproduce satisfactorily the properties of transition metal alloys [15, 25] and, rather unexpectedly, those of noble metals [15,17].

Limitations

Atomistic simulations suffer from several limitations the causes of which are:

- Potential imperfections
- Time scale
- Space scale

These influence seriously the quality of the results and have to be seriously examined in order to guarantee the validity of the simulation. Potential imperfections are peculiar to the model of cohesive energy that is used and are in principle well known. Their consequences have to be established in detail by comparing simulation results and experimental data e. g. melting point, defect formation enegy, surface relaxations... No perfect model is available and therefore, although sometimes simulations lead to very realistic results, the conclusion still have a more or less pronounced generic character.

As has been already mentioned above, the time step in MD simulations is chosen equal to a fraction of the inverse maximum vibrational frequency in the cristalline state of the studied material. Given the performances of nowadays computers, the maximum number of iterations for the integration of the equations of motion equals 10^7 or, equvalently, the real time duration of the simulation amounts, $\delta T \approx 1$ ns. Thus, phenomena having relaxation times larger than this limit cannot be studied using MD. An example is provided by diffusion processes involving complex defects or the emission in the bulk of point defects from sources such as surfaces, grain boundaries or dislocations. The vibrational properties of the simulated system are also affected since the propagation of phonons cannot be studied when their frequency is lower than a critical cutoff related to the above limit. Finally, phase transitions implying bulk diffusion may not be observed in MD simulations, even if the model includes surfaces or other possible sources of point defects. This limitation can be bypassed using instead MC simulations where the result of diffusion, i. e. the exchange of atoms, can be incorporated in the Markov chain [15].

The spatial scale is an additional limitation which interferes with the time scale problem. Indeed, the larger is the simulated system, the larger is the CPU time per MD step/MC move. The real time duration of the computer "experiment" in MD or the statistical accuracy in MC are greatly affected by the system size. Given that there is no mean to simulate a physical system containing a number of atoms of the order of Avogadro number, periodic boundary conditions (PBC) are usually employed to avoid surface effects. The latter are known to affect the phase diagram of small systems with respect to the bulk [26]. However, in a system with fixed linear dimensions, L, and PBC, a cutoff is introduced in the phonon dispersion since no vibrations corresponding to a wave length, $\lambda \geq \lambda_{max} \approx L$ can propagate in the simulation box. Similarly, collective displacements of atoms may be artifacts rising from unphysical interactions between the simulation box and its periodic images. As a consequence of the above remarks, the mean square displacements (MSD) of atoms are size dependent and convergence to the thermodynamical limit values appears only for systems

containing, N≥2000 particles [17]. It is worth to emphasize on this result since MSD are often used in validations of potential models by comparing them to experimental values obtained from neutron scattering. Such comparisons intend to establish that the potential is well behaved at temperatures different from T=0 K and that the expected melting point of the model is not very different from the experimental value.

In the specific case of grain boundaries, PBC impose the presence in the simulation box of two defects being one the mirror image of the other. According to St Venant's principle, the perturbation due to a grain boundary extends into the bulk over a distance characterictic of its periodicity. Thus, in order to preserve in the simulated system a bulk-like region, its linear dimension along the direction normal to the interface should equal at least six times the characteristic length associated to the periodicity of the defect [27]. In addition, the constraints introduced by the PBC correlate the behavior of the two interfaces e. g. with respect to gliding and migration.

The recent development of antisymmetric, Möbius-like, boundary conditions applied to the study of grain boundaries is an interesting solution allowing for a reduction of the computational cost and allowing for the study of an isolated defect [28].

II. The mesoscopic scale

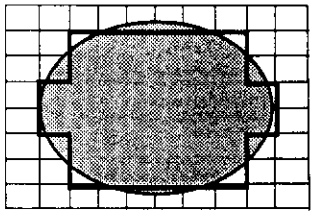

Figure 2 - Mesoscopic scale simulations: discretization of dislocation lines using exclusively screw and edge in character segments.

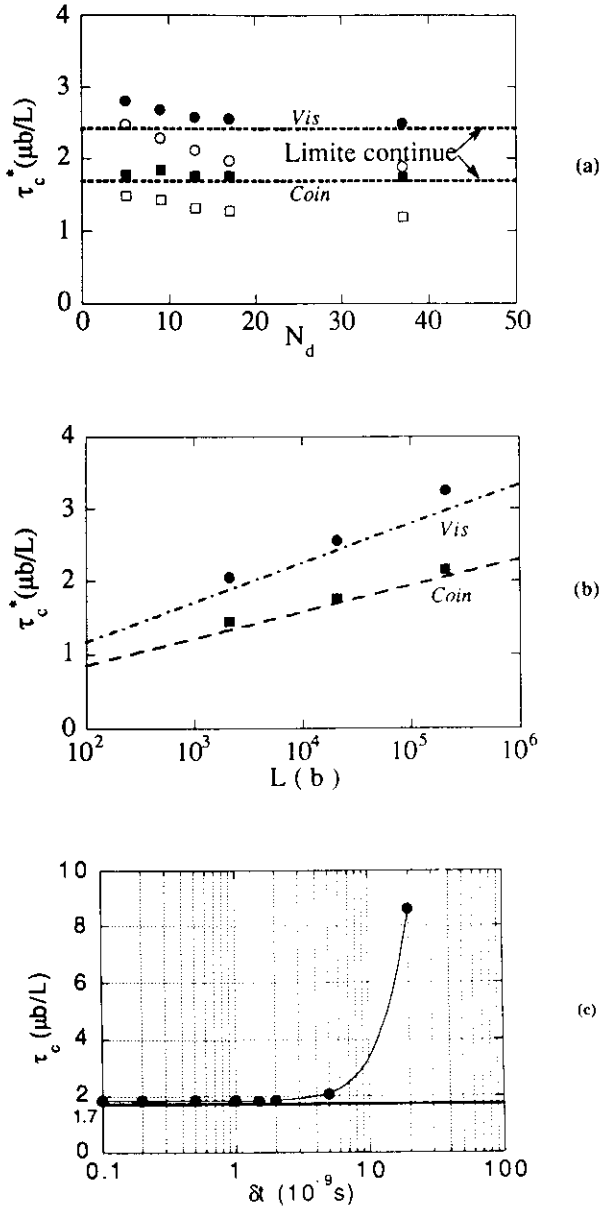

Figure 4 - Mesoscopic scale simulations: Validation of the discretization model (a, b) and of the time step adopted (c) (courtesy B. Devincre).

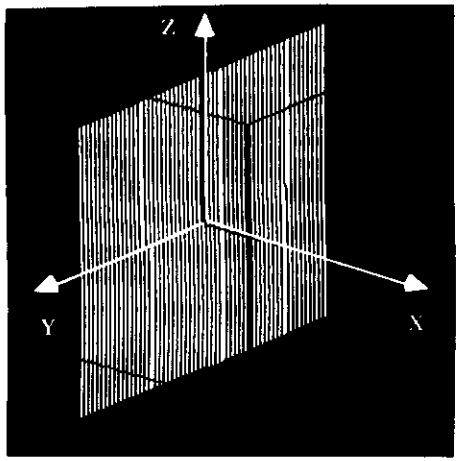

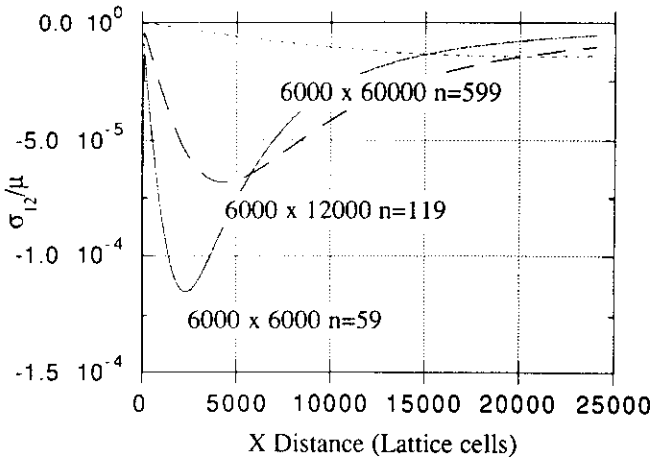

Figure 5 - Mesoscopic scale simulations: intermediate range shear stress generated by subboundaries due to finite extension effects.

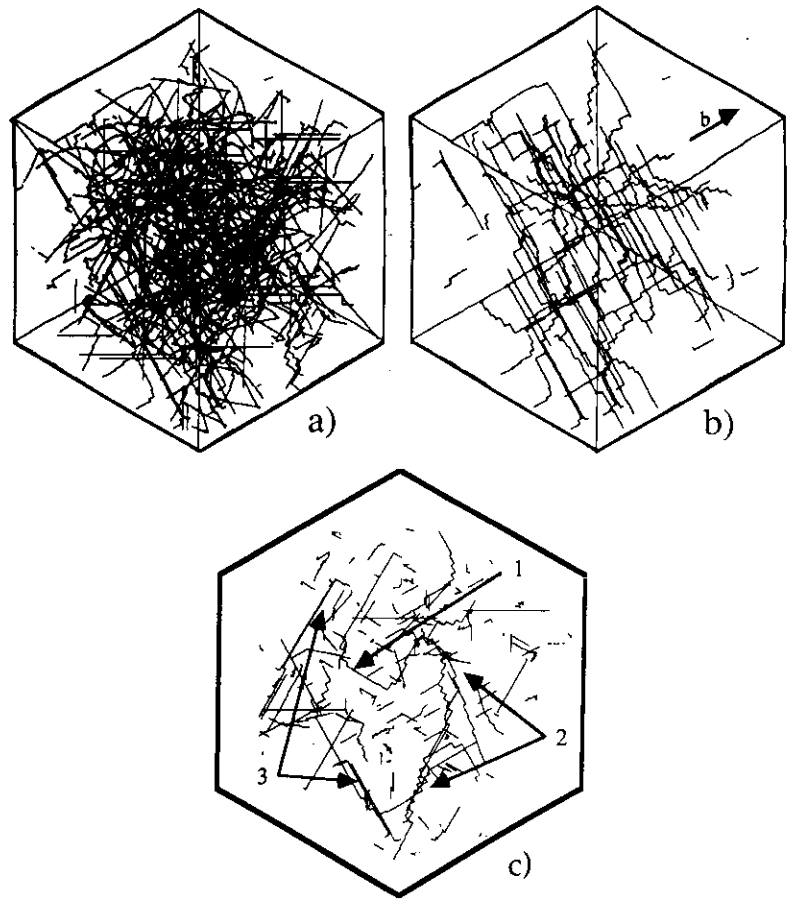

Figure 6 - Mesoscopic scale simulations: (a) projection along a [111] direction of a crystal stressed under multiple glide conditions, after a cumulated deformation at an imposed deformation velocity, ε=0.1%, under . The total dislocation density amounts, $\rho \approx 8 \cdot 10^{11}$ m^{-2}, (b) Same but only 1/2 [101] Burgers vector dislocations are imaged (c) : thin foil (e=0.5 μm). Arrows indicate 1) the position of a dislocation source 2) the position and 3) dislocation dipoles (Courtesy B. Devincre).

III. Simulation results

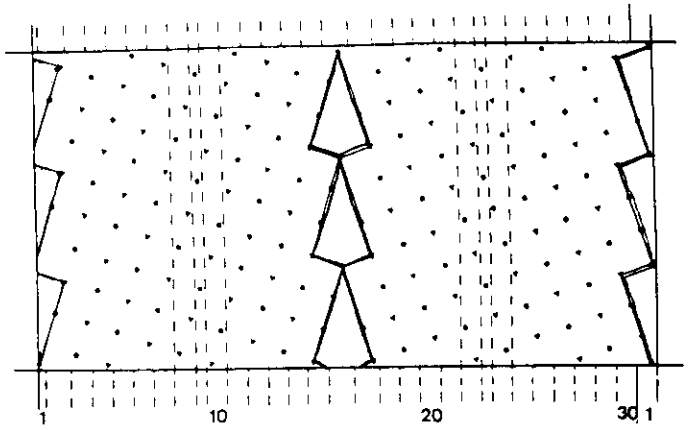

$$A(\vec{r}) = \left\langle \sum_i A_i(\vec{r}_i, \vec{p}_i)\ \delta(\vec{r} - \vec{r}_i) \right\rangle$$

A_i :

- 1 — density $\rho(\vec{r})$
- $\frac{1}{2} \sum_{j \neq i} u(r_{ij})$ — potential energy $U(r)$
- $\frac{1}{3} \left(\frac{p_i^2}{2m} - \frac{1}{2} \sum_{j \neq i} r_{ij} \frac{\partial u(r_{ij})}{\partial r_{ij}} \right)$ — pressure $P(r)$
- $\frac{1}{\rho(r)\rho(r+r')} \sum_{j \neq i} \delta(\vec{r} + \vec{r}' - \vec{r}_j)$ — RDF $g(r)$

$$A_\ell = \frac{1}{V_\ell(\ell)} \int_{V(L)} \left\langle \sum_i A_i\ \delta(\vec{r} - \vec{r}_i) \right\rangle d\underline{r}$$

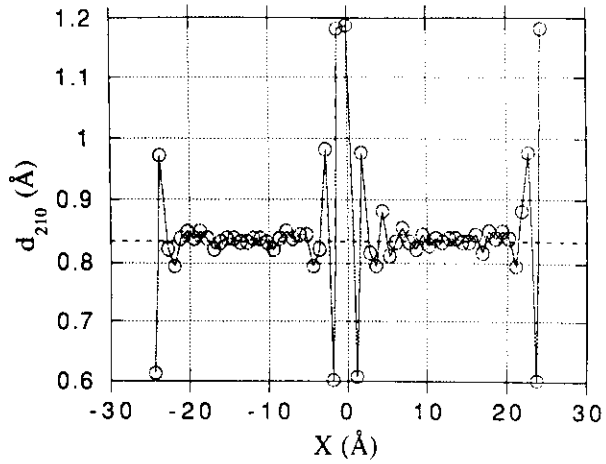

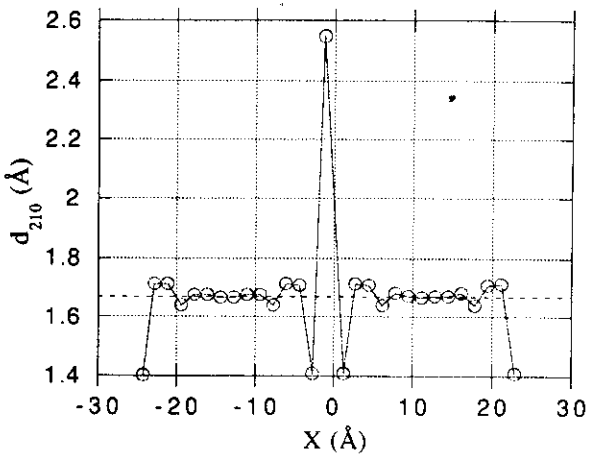

Figure 7 - Static relaxations of atomic planes parallel to a Σ=5 (210) [001] tilt boundary in Cu_3Au. (a) : copper planes (b) : gold containing planes.

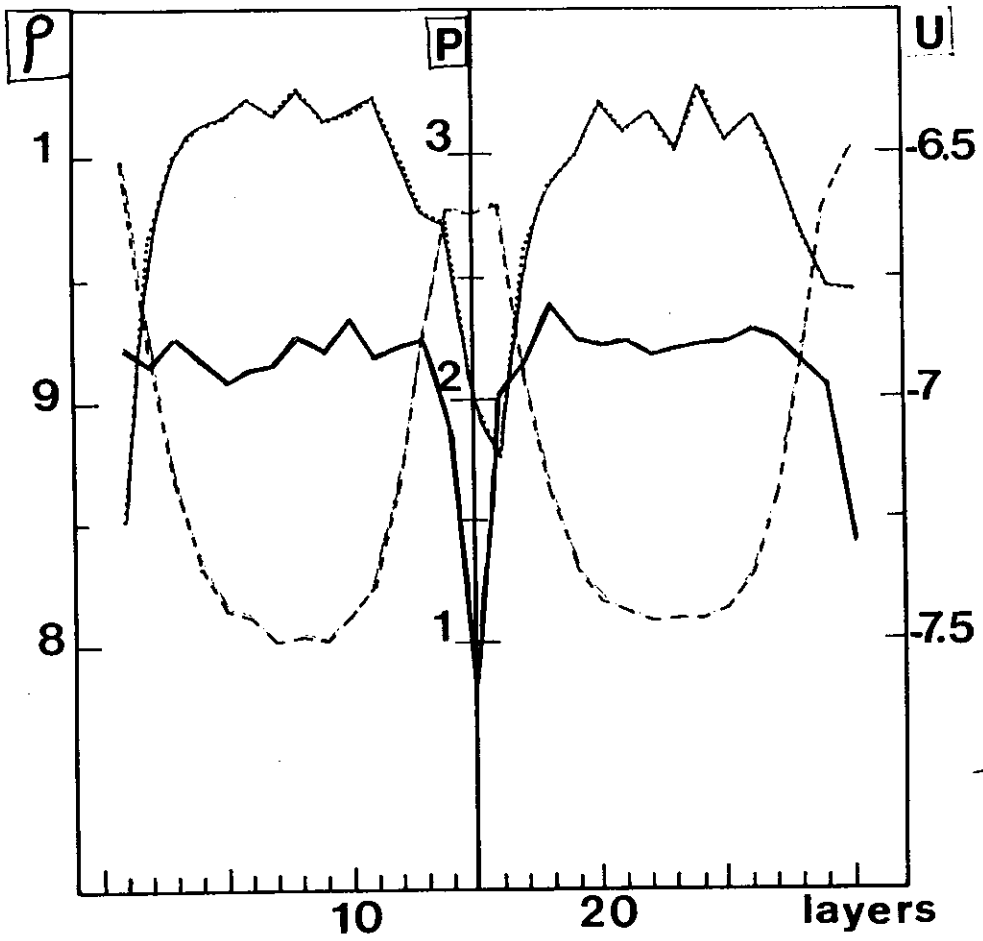

$T = 0.7\ (\tau T_m)$

ccolti et al. (1983) LJ (12-6) $\Sigma = 5$ (310) [001] tilt, Reduced units

⊗ Dynamical properties: $\langle u^2 \rangle_{bulk}$ vs. $\langle u^2 \rangle_{GBy}$

Dagens (1973, 1975), pseudopotential for noble metals

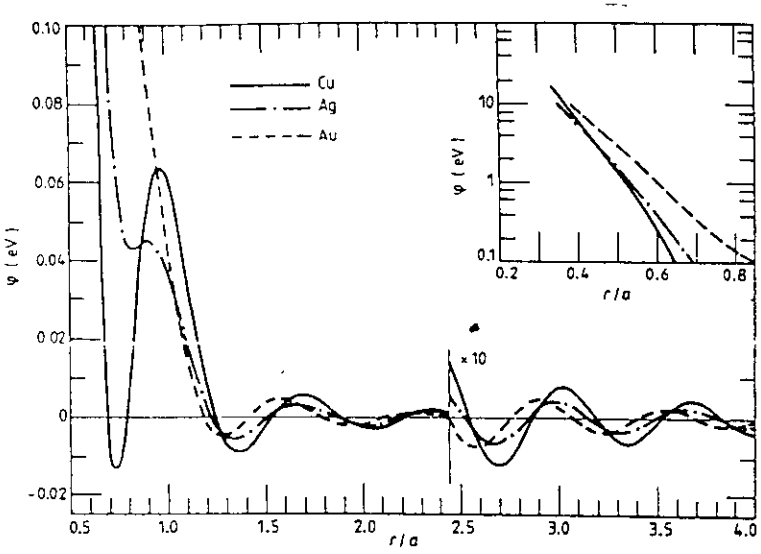

- C_{11}, $C_{12} = C_{44}$
- Formation and migration energies of point defects.
- Bulk $\langle u^2 \rangle$

MD (NVT) - Nosé

$\Sigma = 13$ [001] $\theta \sim 22.6°$ Ag, Au, Cu.

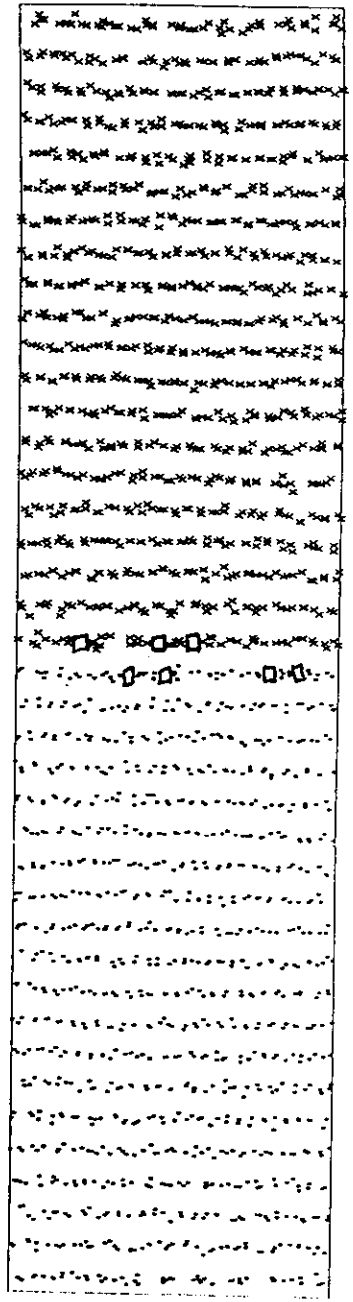

⊗ [010]

[510]

X ⟶ [001]

Au XYTJ 1250/2000 pas

Local evaluation of $\langle u^2 \rangle = f(x, T)$

T=0K

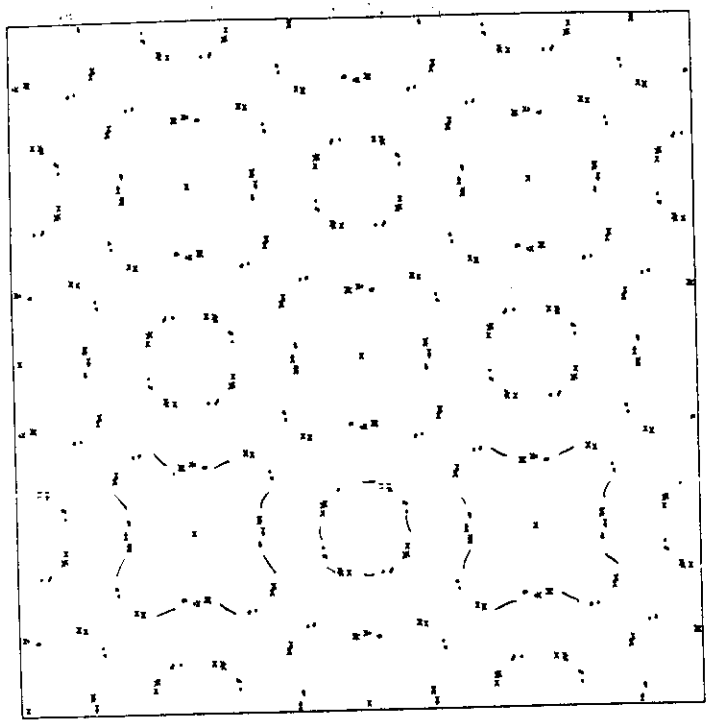

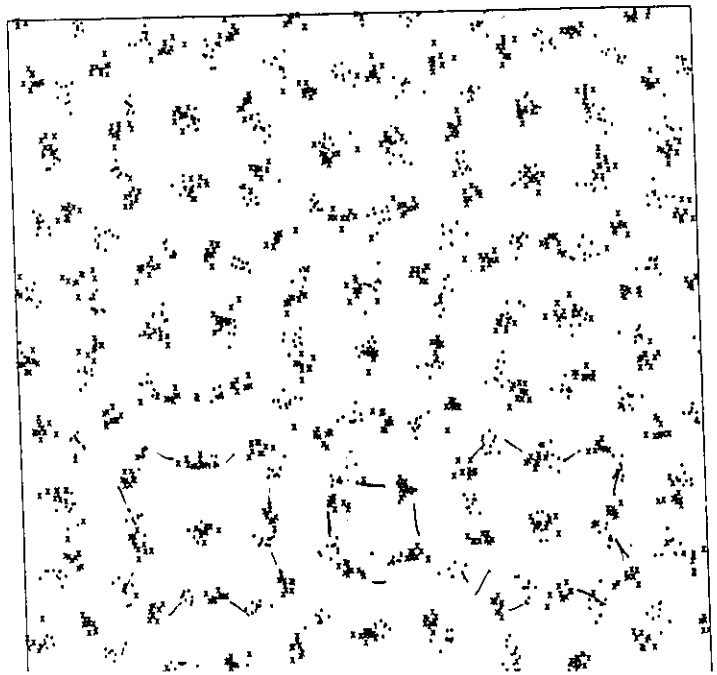

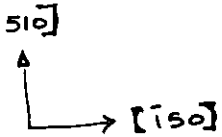

⊗ [001]

◍ Gby $\langle u^2 \rangle$ are larger than bulk $\langle u^2 \rangle$

Same as in the case of : surfaces
dislocations
tilt boundaries → practicals

Premelting effects ?

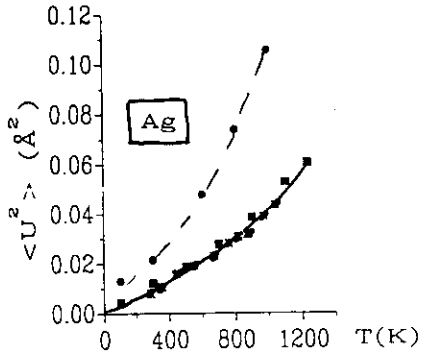

(a)

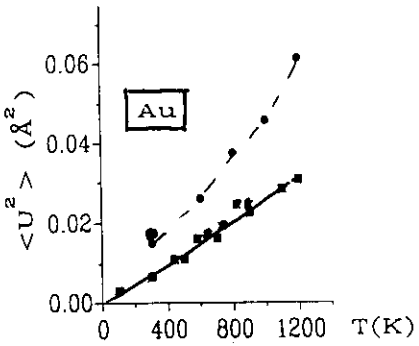

(b)

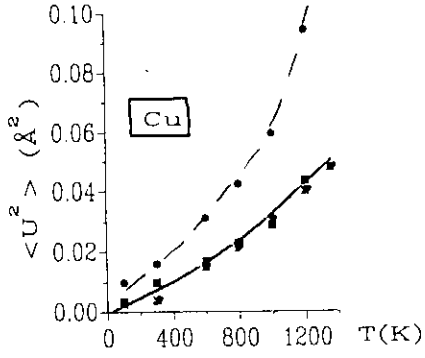

(c)

Fig. 3 - Bulk and grain boundary MSD temperature dependence for : (a) Ag, (b) Au and (c) Cu. Full squares (■) : MD data, asterisks (✳) : experimental values /18,19/, full dots (●) : MD data in the grain boundary core.

- Synchrotron, Fitzsimmons et Sass, PRL (1988)
- Evangelakis et al., J. de Physique, Paris, 51, C1-127 (1990)

- Frenkel pair creation by migration of an A or B site atoms to an I location.
- Multiple jumps

$\Sigma = 5$ (210) [001]

LJ (12-6)

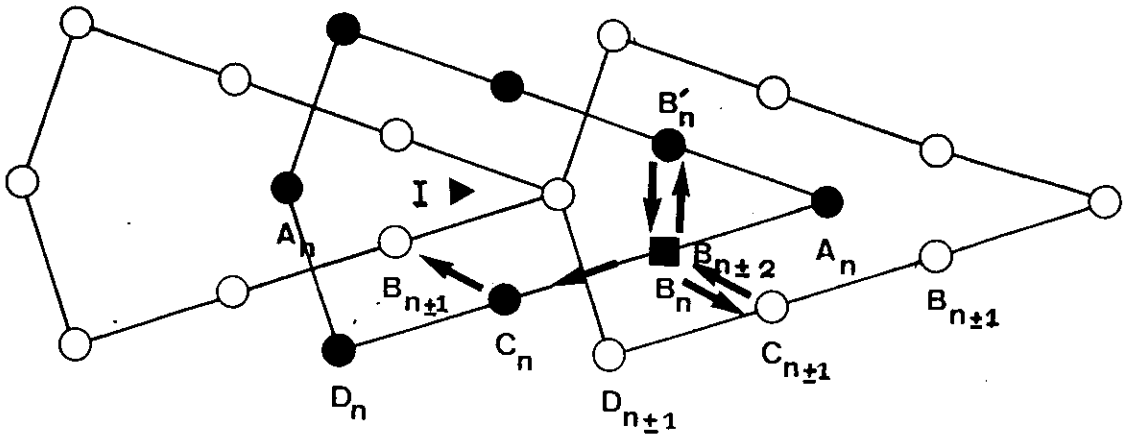

- Dissociation of the Frenkel pair by the vacancy migration, the interstitial remaining immobile → Dominance of the vacancy mechanism for intergranular diffusion.

- Crystalline features of Gby diffusion

T. Kwok PhD (1986)

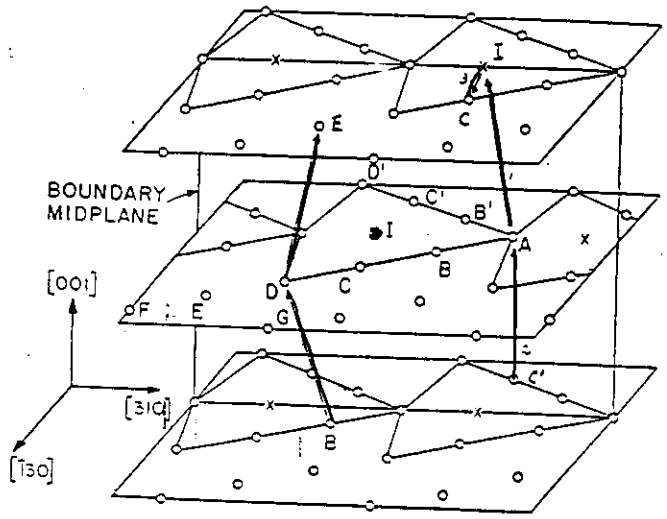

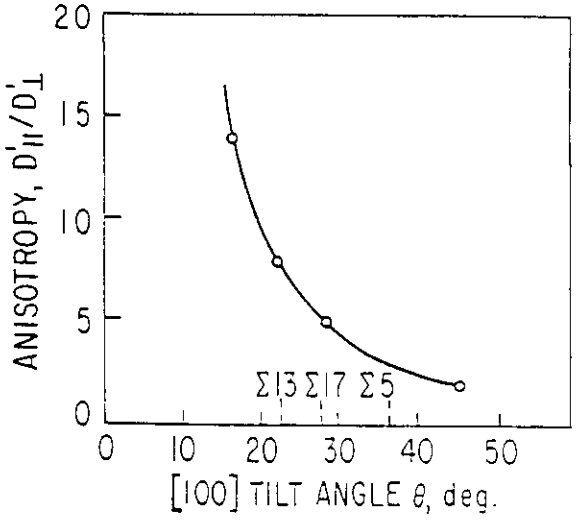

High D : E_F decreases (up to 50%)

Multiple jumps

Is diffusion 'liquidlike' ?

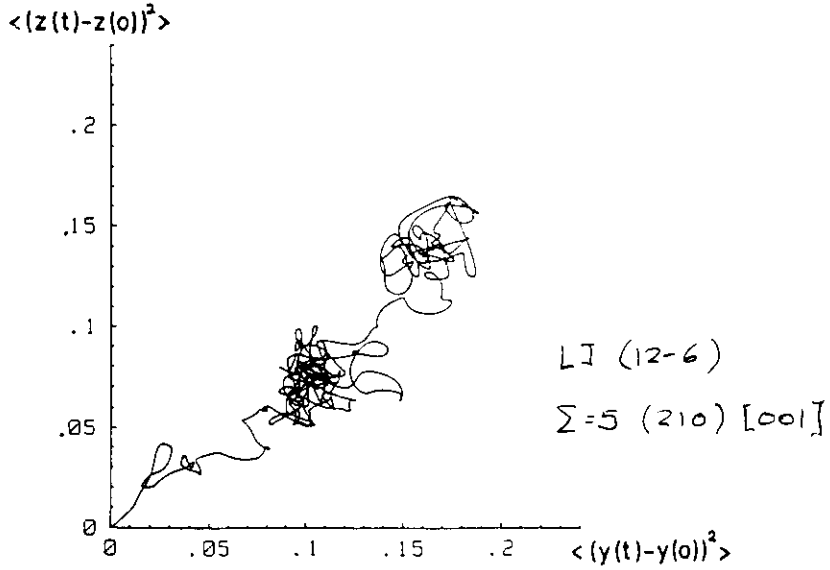

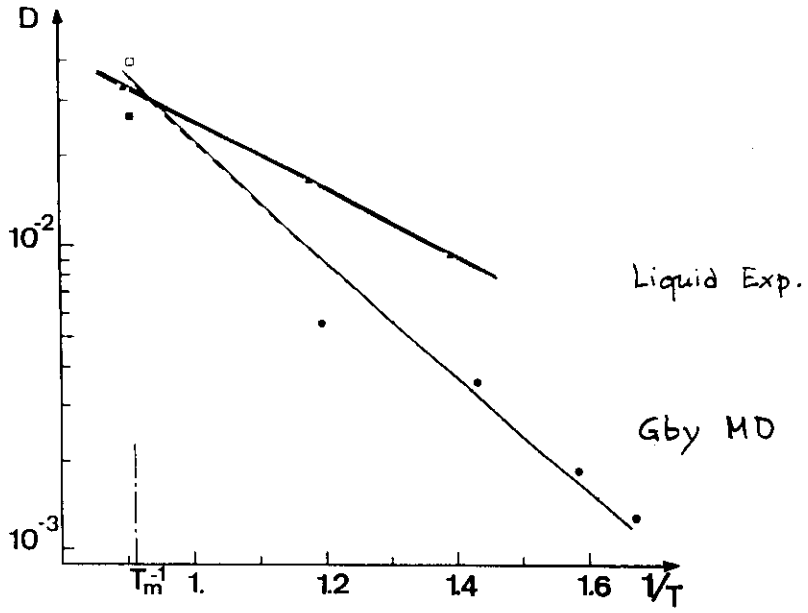
D
10^{-2}
10^{-3}
T_m^{-1}
1.
1.2
1.4
1.6
$1/T$
Liquid Exp.
Gby MD

Premelting effects ?

$$\rho_k^{\ell} \equiv \int_{V_\ell} \left\langle \sum_i \delta(\vec{r}-\vec{r}_i) \right\rangle e^{-i\vec{k}\vec{r}}\, d\vec{r} = \sum_{i\in\ell} e^{-i\vec{k}\vec{r}_i}$$

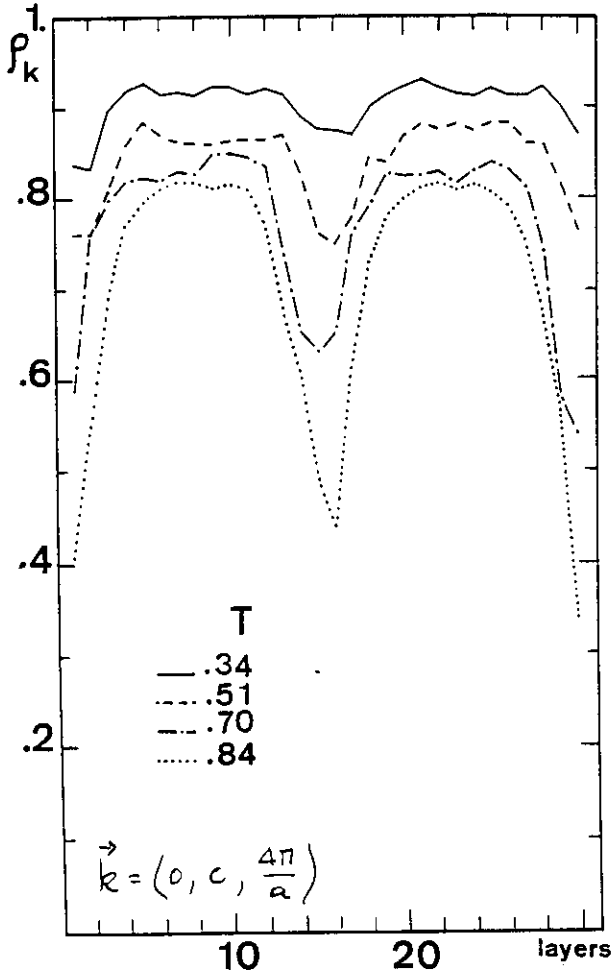

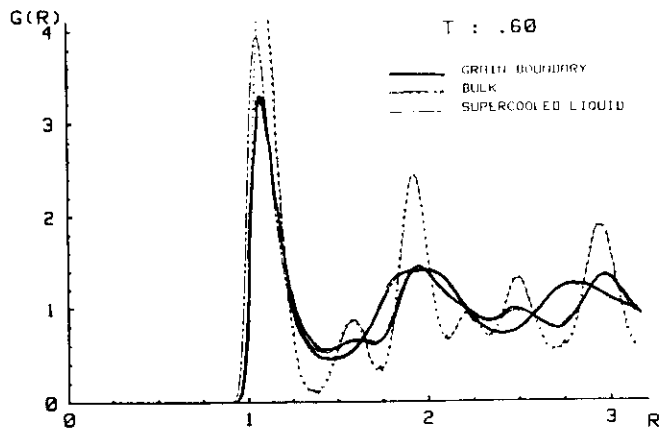

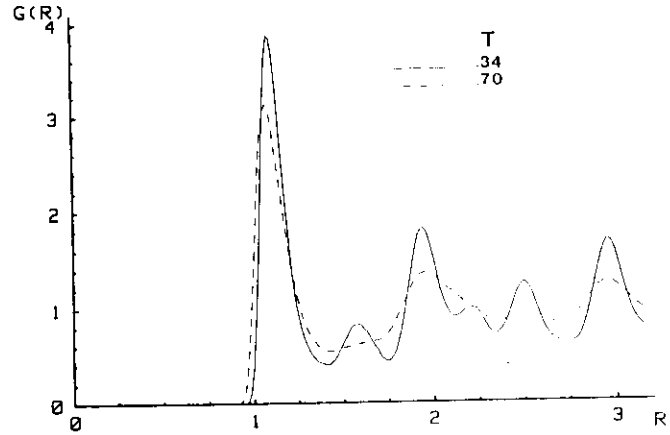

Localized, liquidlike disorder ≠ melting!

Solid : $f_k = N$

Liquid : $\rho_k = 0$ (amorphous)

- A temperature-induced φ-transition

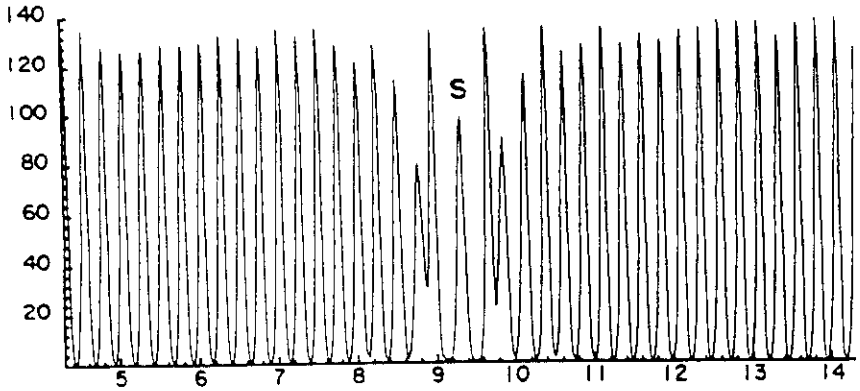

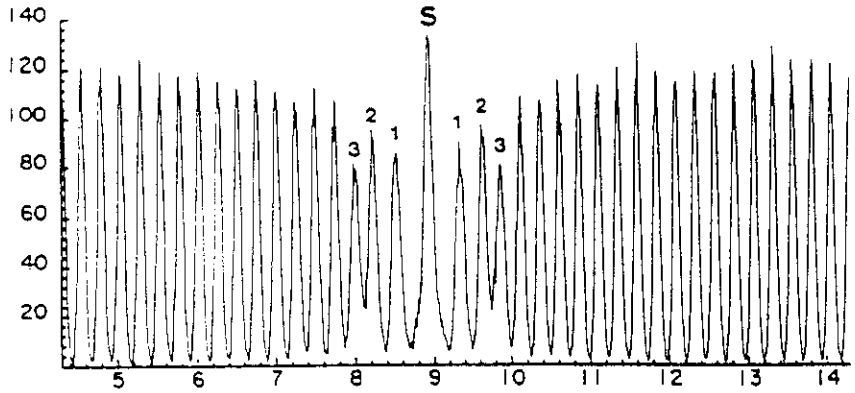

- $\Sigma=5$ (210) [001], LJ ($\varepsilon=119.8\,K$, $\sigma=3.405\,\text{Å}$)
  $N=1280$ atoms, PBC $8\times[210]\times 2\times[\bar{1}20]\times 4\times[001]$

- $\rho_{[210]} = \left\langle \sum_i \delta(x-x_i) \right\rangle$

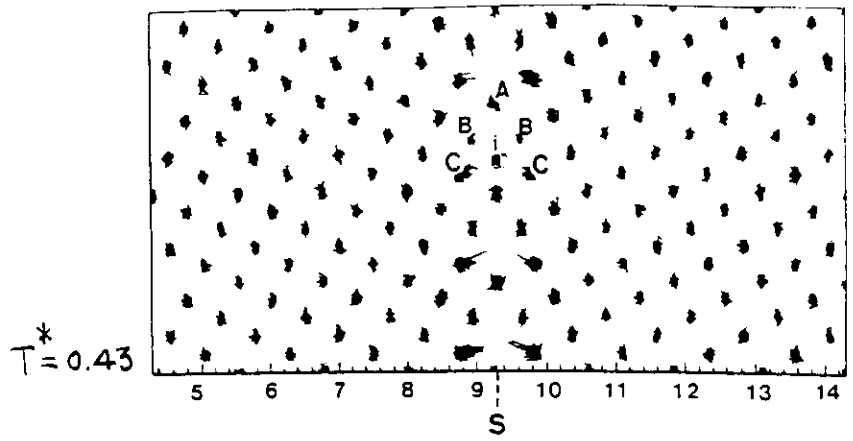

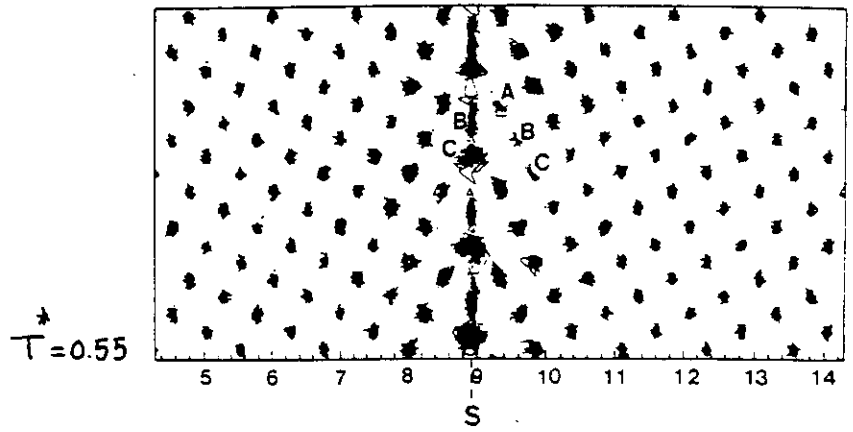

Entropy is responsible

Mecanism:

Coupled migration-
rigid body tr.

Segregation?

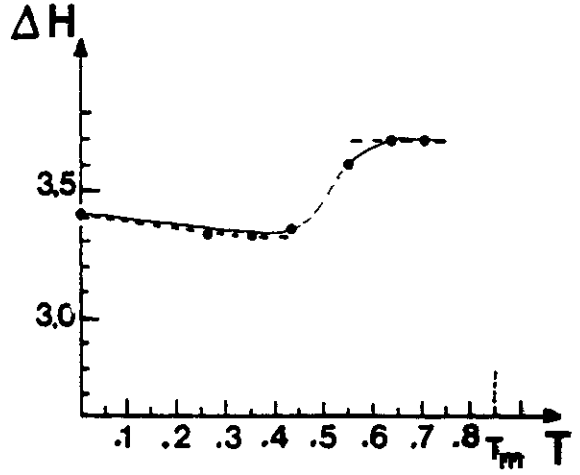

cf. Vitek et al., J. Physique, 46, C4-171 (1985)

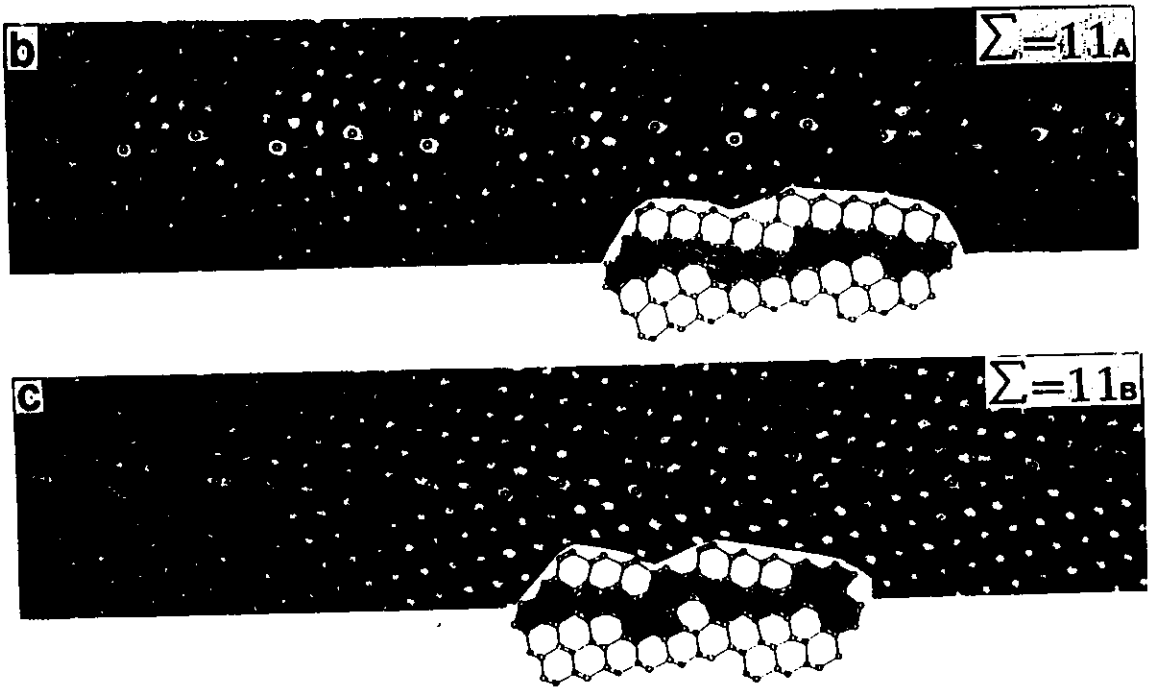

- $\Sigma=9$ $(\bar{1}2\bar{2})$ $[011]$ deformation $\varepsilon \simeq 6.8\%$ $\longrightarrow$ $\Sigma 187, 11, 41 \ldots$
- (b) $M^+ I^- M^- I^-$ $\longrightarrow$ (c) $M^+ I^- M^- P^+ M^- I^- M^+ P^-$
- Temperature induced φ-transition or dislocation mediated structural change

J.L. PUTAUX - J. THIBAULT, J. Physique, 51 (1990) C1-323

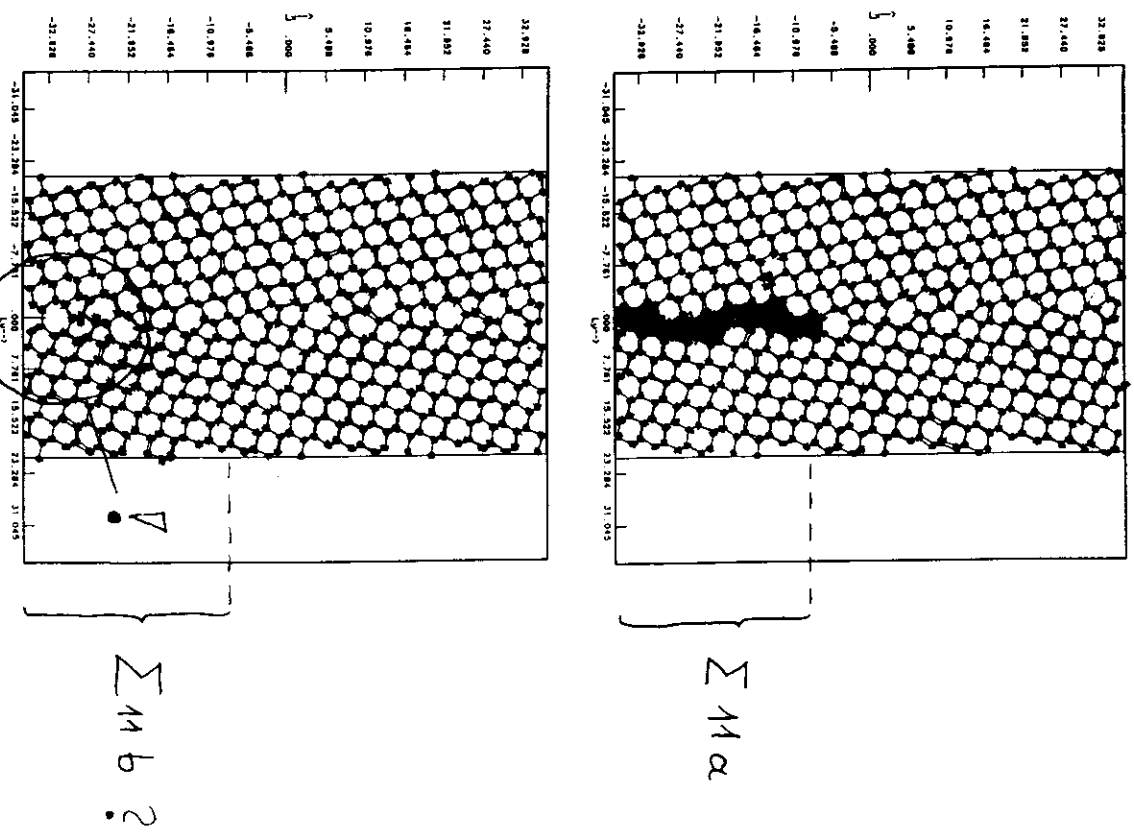

- Tersoff (c) potential
- $T \simeq 2050$ K, Möbius BC
- $\Sigma 11a$ - $\Sigma 11b$ correspond to # rigid body translations

O.H. Dupare, (1993), in preparation.

(rigid body translations ...!)

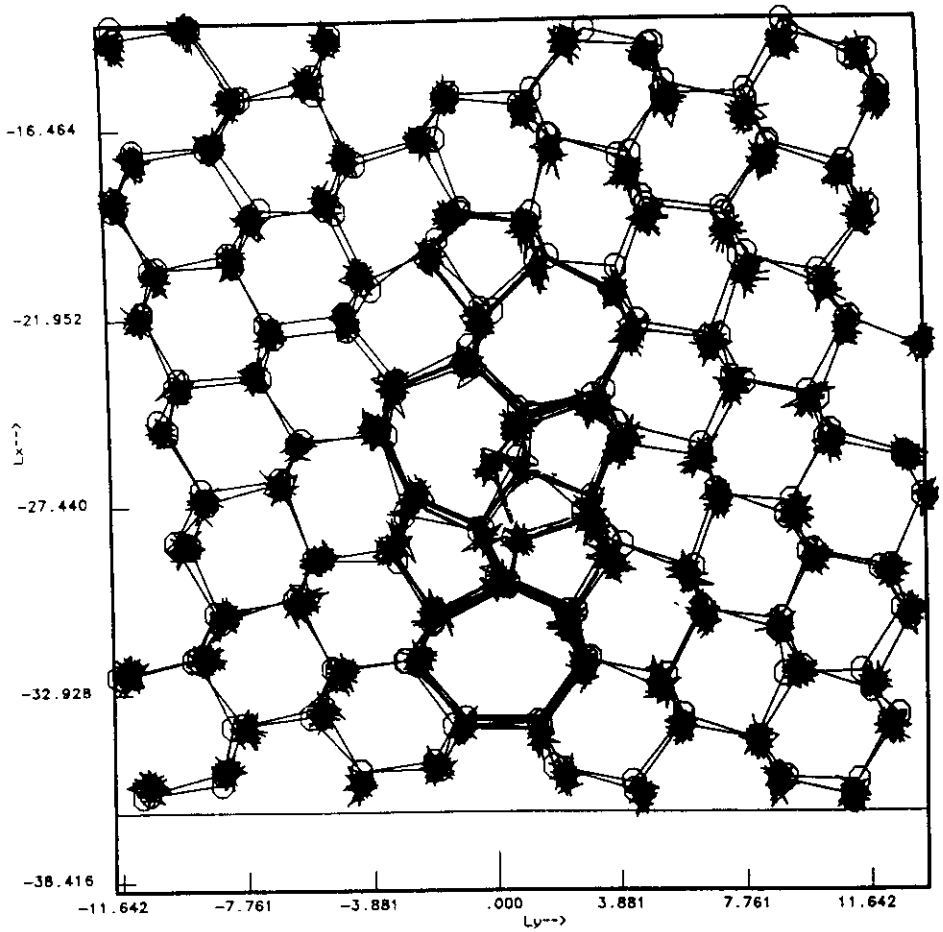

- $\Sigma 11$ b is stabilized by lattice dislocations.

O.H. Dupare, (1993) in preparation

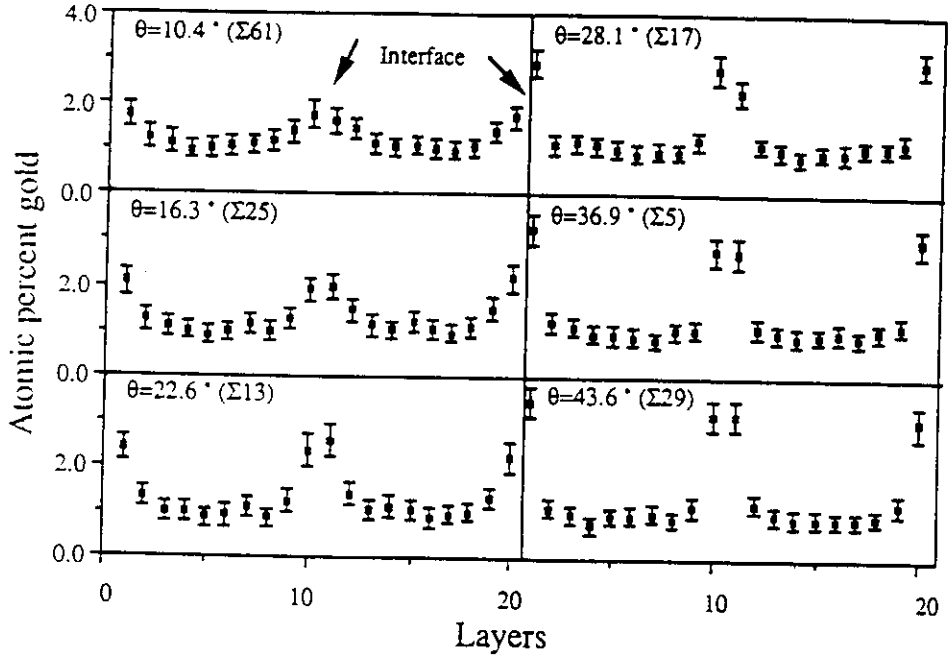

Fig. 3. The concentration of gold (at.%) in the (002) planes *vs.* the distance normal to the interface for $\theta = 10.4°$ ($\Sigma = 61$), $\theta = 16.3°$ ($\Sigma = 25$), $\theta = 22.6°$ ($\Sigma = 13$), $\theta = 28.1°$ ($\Sigma = 17$), $\theta = 36.9°$ ($\Sigma = 5$), and $\theta = 43.6°$ ($\Sigma = 29$) (001) twist boundaries. The interfaces are indicated by arrows. There is more than one interface present because of the periodic boundary conditions employed. The concentrations are averaged over $(3-5) \times 10^6$ Monte Carlo steps and the error bars have a total length equal to four standard deviations.

Scidman, Mat. Sci. Eng., A137, 57, (1991). -42-

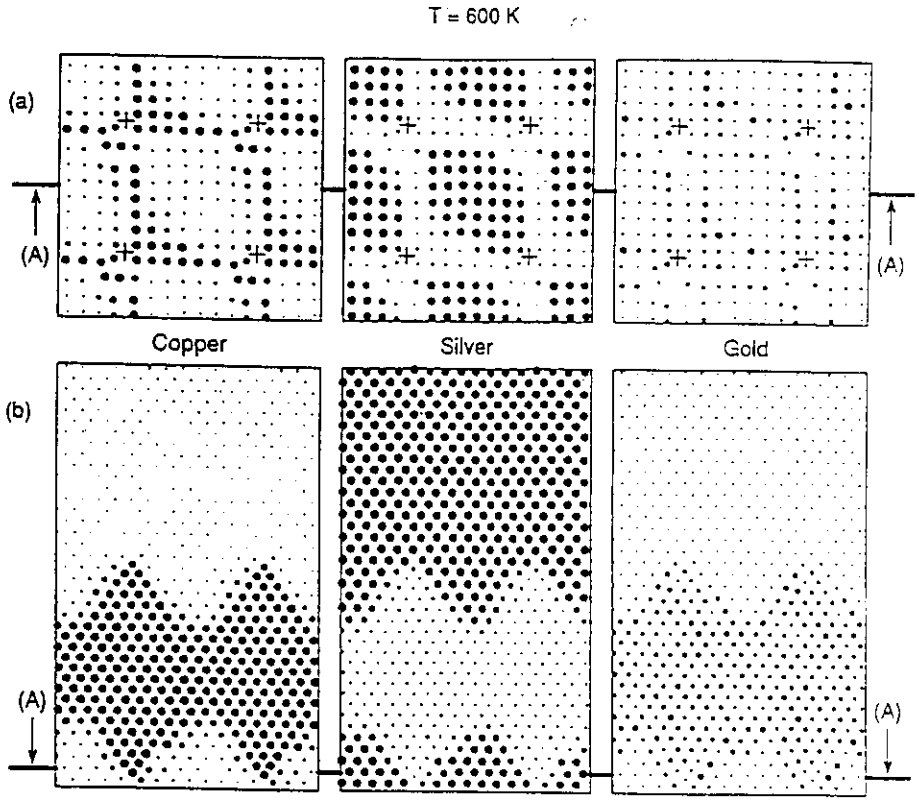

Fig. 7. Statistical distribution of Cu, Ag and Au atoms obtained at 600 K along two cross-sections of the interfacial computational cell: (a) the 2nd layer parallel to the initial interface plane, in the Cu-rich phase, and (b) projection of two atom planes perpendicular to the interface plane, and passing through the points of coincidence. There are two periodic lengths along the horizontal axis, and two periodic lengths in (a) and only one in (b) along the vertical axis. The thick lines labelled (A), represent the intersection between the two cross sections. The size of each atom is scaled to the probability of finding a particular atom species at a given site. The sizes of Au atoms have been scaled up by a factor of 1.5, compared to the two other species.

BACHER, WYNBLATT, FOILES, Acta Met. 39, 2681 (1991)
-43-

● Heterophase interfaces

Why are they important ?

- Magnetic properties

$\frac{1}{3}(n, n)$

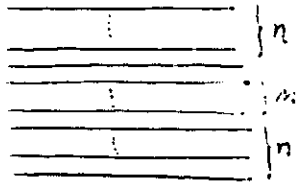

- protective coatings (oxydation, corrosion ...)

- Solid state reactions (interdiffusion, amorphization ...)

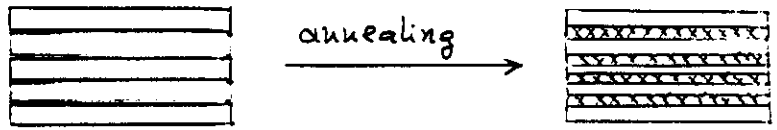

cristal

possibly amorphous !

Johnson W.L, Prog. in Mater. Sci, 30, 81 (1986) Review

Weissmann et al, Phys. Rev., B46, 2577 (1992) MD

The Ni-Zr interface.

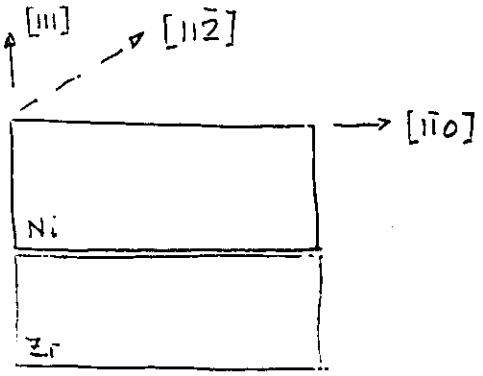

$$d^{Ni}_{[110]} \cdot n^{Ni} \approx d^{Zr}_{[110]} \cdot n^{Zr}$$

Approximate solutions

n^{Ni}	n^{Zr}	res. misfit
→ 9	7	1.1×10^{-2}
13	10	3.3×10^{-3}
⋮	⋮	⋮
271	209	9.3×10^{-6}

81 atoms Ni
49 " Zr
} per plane

Atomic relaxations → minimum el. energy

N-body potential.

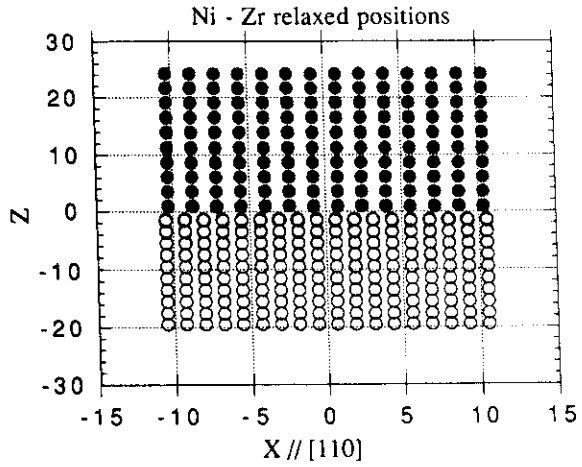

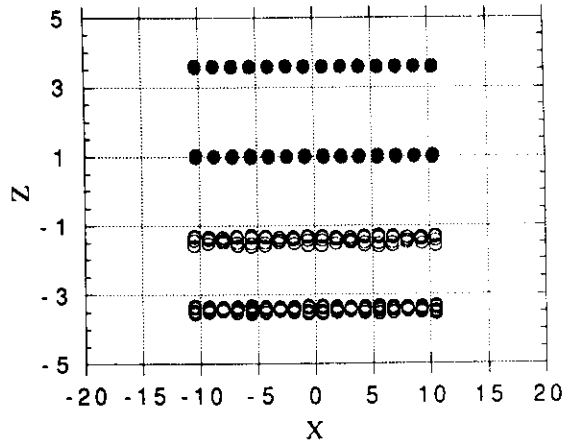

Figure 8 - A relaxed Ni-Zr interface. The lower part of the figure is a magnification of the region close to the interface. Atomic relaxations are larger in the Ni part of the bilayer.

Heterophase interfaces (cristal-amorphous)

Chemical disorder in some intermetallic compounds ⟶ amorphization

Ex: $NiZr_2$

Massobrio et. al., Phys. Rev. Lett., 62, 1142 (1989)

Chemical disorder occurs under: irradiation
mechanical alloying.

Amorphization is closely related to anelastic deformations due to differences in atom "size"

Massobrio et al., Phys. Rev., B45, 2484 (1992)

Question:

Is the C-A reaction related to a nucleation-growth process?

A C-A interfacial properties study is needed!

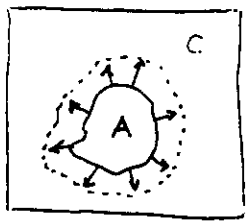

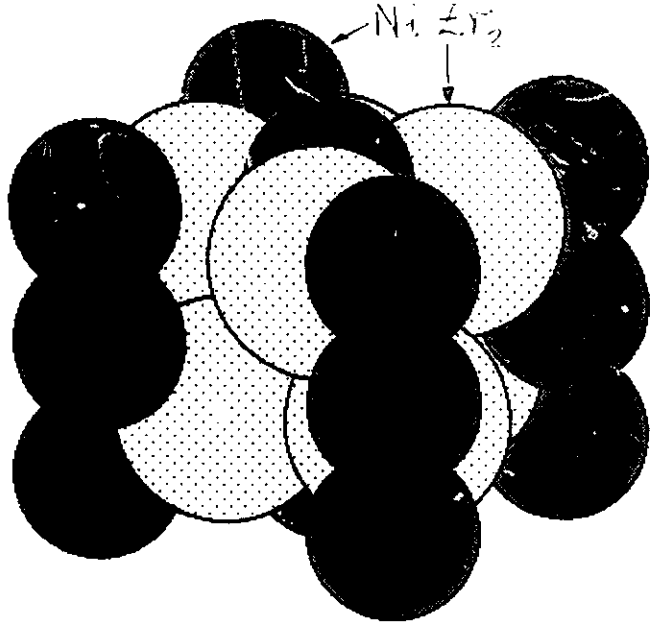

$$\rho(x) = \left\langle \sum_i \delta(r - r_i) \right\rangle$$

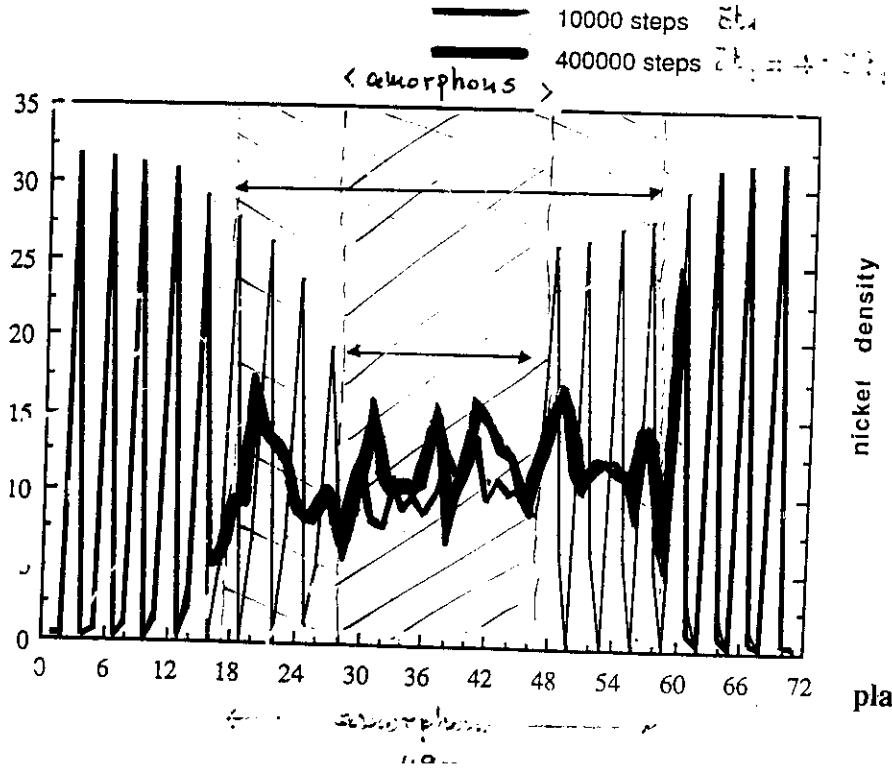

IV. Conclusion and perspectives

● Conclusion - Perspectives

- Parallel investigations of Gb's properties using HREM and computer simulation (identical scales, model validation)
- Studies of general boundaries are needed
- Coupling of "micro-meso" scales

● Open questions

Mechanical properties

Interaction Gby - lattice dislocations

Influence of the composition

Glide and sliding mechanisms ?

⇓

INTERFACE ENGINEERING !

V. References

I. Introduction to MC-MD techniques

[1] Fermi E., Pasta J. and Ulam S., Los Alamos Report n° LA - 1940 (1955).

[2] Alder B. J. and Wainwright T. E., J. Chem. Phys., **27**, 1208 (1957); **31**, 459 (1959).

[3] Gibson J. B., Goland A. N., Milgram M. and Vineyard G. H., Phys. Rev., **120**, 1229 (1960).

[4] Verlet L., Phys. Rev., **159**, 98 (1967).

[5] For a brief historical overview of contributions in the field see also:
Hansen J. P., in "Computer Simulation in Materials Science: Interatomic potentials, Simulation techniques and Applications", M. Meyer and V. Pontikis Eds, NATO ASI Series E: Applied Sciences, vol. 205, p. 3 (1991) (Klewer, Amsterdam).

[6] Reif F., "Fundamentals of Statistical and Thermal Physics", (1965) (McGraw, New York).

[7] Valleau J. P., p. 67 in ref. [5].

[8] Allen M. P. and Tildesley D. J., "Computer Simulation of Liquids", 1987, (Oxford university press, Oxford).

[9] Metropolis N., Rosenbluth A. W., Rosenbluth M. N., Teller A. H. and Teller E., J. Chem. Phys., **21**, 1087 (1953).

[10] Frenkel D., p. 85 in ref [5].

[11] Nosé S., J. Mol. Phys., **52**, 255 (1984).

[12] Andersen H. C., J. Chem. Phys., **72**, 2384 (1980).

[13] Parrinello M. and Rahman A., J. Appl. Phys., **52**, 7182 (1981).

[14] Loisel B., Gorse D., Pontikis V. and Lapujoulade J., Surface Sci., **221** (1989) 365-378.

[15] Rey-Losada C, Hayoun M. and Pontikis V., J. Mater. Res., **291**, 549 (1993).

[16] Loisel B., Lapujoulade J. and Pontikis V., Surface Sci., **256**, 242 (1991).

[17] Rosato V., Guillopé M. and Legrand B., Phil. Mag., **59**, 231 (1989).

[18] Car R. and Parrinello M., Phys. Rev. Lett., **55**, 2471 (1985).

[19] Daw M. S. and Baskes M. I., Phys. Rev., **B29**, 1285 (1984).

[20] Ducastelle F., J. Physique, Paris, **31**, 1055 (1970).

[21] Finnis M. W. and Sinclair J. E., Phil. Mag., **A50**, 45 (1984).

[22] Masuda K. and Sato A., Phil. Mag., **37**, 531 (1978).

[23] Evangelakis G. A., Rizos J. P., Lagaris I. E. and Demetropoulos I. N., Comp. Phys. Comm., **46**, 401 (1987).

[24] Willaime F. and Massobrio C., Phys. Rev., **B43**, 11653 (1991).

[25] Massobrio C., Pontikis V. and Martin G., Phys. Rev., **B41**, 10486, (1990).

[26] Rosato V., Ciccotti G. and Pontikis V., Phys. Rev., **B33**, 1860, (1986).

[27] Ciccotti G., Guillopé M. and Pontikis V., Phys. Rev., **B27** (1983) 5576-5585.

[28] Hardouin-Duparc, to be published (1993).

II. Mesoscopic scale

[1] Devincre B., PhD, Université Paris XI (1993).

[2] Devincre B., Pontikis V, Bréchet Y., Canova G., Condat M. and Kubin L., in "Microscopic simulations of complex hydrodynamic phenomena", Eds. M. Mareschal and B. L. Holian, NATO ASI Series B: Physics, vol. **292**, p. 413 (1991) (Klewer, Amsterdam).

[3] Devincre B. et Condat M., Acta Metall. Mater., **40**, 2629 (1992).

[4] Kubin L.P., Canova G., Condat M., Devincre B., Pontikis V., Bréchet Y., Solid State Phenomena Vol. **23&24**, 455 (1992).

[5] Kubin L.P., dans "Materials Science and Technology" vol. 6, p. 137, Eds. R.W. Cahn, P. Haasen, E.J. Kramer VCH (Weinheim, FRG), (1992)

III. Survey of simulation results

[1] Balluffi R. W. and Hsieh T. E., J. Physique, Paris, **49**, C5-337 (1988).

[2] Puteaux J. L. and Thibault-Desseaux, J. Physique, Paris, **51**, C1-323 (1990).

[3] Evangelakis G. A., Hou M., Maunier C. and Pontikis V., J. Physique, Paris, **51**, C1-127 (1990) .

[4] Gurgel-Fernandes M. and Pontikis V., in preparation (1993).

[5] Massobrio C. and Pontikis V., Proceedings of the NATO-CECAM workshop on : "Microscopic simulations of complex flows", held August 23-25, 1989, BRUSSELS, Ed. M. Mareschal, Series B: Physics Vol. **236**, p. 297 (Plenum, 1990).

[6] Massobrio C. and Pontikis V., Phys. Rev. **B45**, 2484 (1992).